

PREDICTING GALLOPING AMPLITUDES

By A. S. Richardson, Jr.¹

ABSTRACT: The use of wind tunnel data, lift and drag, together with a method of analysis, leads to estimates of gallop amplitudes. No damping is considered. The nonlinear analysis is similar to the describing-function method used in control system design. The method is convenient to use because it can account for effects of Reynold's number directly. Two bluff body shapes are chosen to illustrate the prediction method. The first shape is the square section. This is also compared with earlier results. The second shape is the simulated ice shape on a round conductor. The results compare favorably with previous work.

INTRODUCTION:

A number of papers have appeared during the past decade that have dealt with the important goal of predicting galloping amplitudes. Mukhopadhyay and Dugundji (1976) reported on experiments and theory for a galloping cantilever beam in two degrees-of-freedom having a square cross section. Later, a method of predicting galloping exposure of transmission line spans was reported (Richardson 1982). In 1983, the maximum amplitude of galloping cables was considered by Ericsson (1983). Recently, the galloping amplitude prediction method (Egbert 1985) has used a control analysis method known as the describing function.

The purpose of this paper is to draw from the earlier prediction methods certain comparisons and to explain a more generalized technique in this instance. Especially, there is found to be evidence of Reynolds number effect on the aerodynamic lift, but little effect on the aerodynamic drag. The technique introduced here shows how to account for such effects in the prediction of galloping amplitude.

GENERALIZED DESCRIBING FUNCTION

The galloping of cables, conductors, beams, masts, etc. is the result of negative aerodynamic damping associated with negative slopes of the normal force coefficient with respect to angle of attack (Parkinson 1965), and while damping is a function of wind speed, a certain minimum wind speed is required to overcome the mechanical damping. Above that wind speed, the galloping amplitude grows at a rate in proportion to wind speed or at a constant dynamic angle of attack. The numerical value of the constant dynamic angle of attack is crucial to the correct prediction of the galloping amplitude. Thus far, the prediction methodology has relied on the somewhat tedious curve-fitting of the aerodynamic normal force function and the establishment of a steady-state oscillatory "galloping condition."

¹President, Research Consulting Associates, Lexington, MA 02173.

Note. Discussion open until September 1, 1988. To extend the closing date one month, a written request must be filed with the ASCE Manager of Journals. The manuscript for this paper was submitted for review and possible publication on October 10, 1986. This paper is part of the *Journal of Engineering Mechanics*, Vol. 114, No. 4, April, 1988. ©ASCE, ISSN 0733-9399/88/0004-0716/\$1.00 + \$.15 per page. Paper No. 22398.

The energy input from the wind to any system undergoing cross-wind oscillation in a single-degree-of-freedom is found by integrating the components of lift and drag over a complete cycle:

$$E = \frac{qA}{\Omega} \int_0^{2\pi} (C_L \cos \alpha + C_D \sin \alpha) \times \frac{dy}{dt} \times d(\Omega t) \dots \dots \dots (1)$$

where q = dynamic pressure; A = reference area for the coefficients C_L and C_D ; Ω = radian frequency of the oscillation; α = instantaneous angle of attack; y = vertical dynamic displacement; and t = time. The instantaneous angle of attack and the displacement are related: $dy/dt = -\Omega Y \sin \Omega t$; and $\alpha = a \sin \Omega t$.

It is seen that the angle of attack and transverse velocity of motion are out of phase (180°). It is precisely this connection that leads to the Den Hartog criterion, i.e., when the slope of the lift coefficient versus angle of attack is negative and is more negative than the drag coefficient is positive, then instability is possible. This applies to small dynamic angles of attack ($a \ll 1$), however. If large dynamic angles of attack occur, such as for values of the a -parameter near unity, then nonlinear behavior of the aerodynamic coefficients C_L and C_D become evident. In general, this means that both C_L and C_D are best represented by their Fourier series components in the interval of one vibration cycle. For large values of a , many harmonic terms may be required to accurately represent the coefficients.

The simplest representation is to assume C_D constant and C_L as

$$C_L = C_0 + S_1 \sin \Omega t + C_1 \cos \Omega t \dots \dots \dots (2)$$

where C_0 , S_1 , and C_1 = the Fourier coefficients.

Under that simplifying assumption the energy input per cycle to the oscillation is found by substituting Eq. 2 into Eq. 1 as follows:

$$\frac{E}{qAY} = -S_1(J_0 - J_2) - 2C_D J_1 \dots \dots \dots (3)$$

Whenever $E > 0$, energy is taken into the system from the wind, causing the system to vibrate at larger amplitude. Whenever $E < 0$, energy is taken out of the system by the wind, causing the system to vibrate at lesser amplitude. The balance condition wherein no net energy flows to or from the wind is the limit cycle oscillation. The equation is the nonlinear equivalent of the Den Hartog criterion, when $E = 0$.

To see this, put the left-hand side equal to zero, and consider only small amplitudes. In that case, $S_1 = (dC_L/d\alpha) a$ and $J_0 = 1$; $J_1 = 0.5 a$; and $J_2 = 0$ (Janke 1945). Therefore, $0 = dC_L/d\alpha + C_D$. This is recognized as the Den Hartog relationship or criterion. When the left-hand side of Eq. 3 is put equal to zero, a single transcendental relationship results with two parameters, the peak angle of attack a and the parameter $R(a)$ defined by

$$R(a)J_1(a) = J_0(a) - J_2(a) \dots \dots \dots (4)$$

where

$$R(a) = \frac{-2C_D}{S_1} \dots \dots \dots (5)$$

The parameter S_1 is the first Fourier series component of lift coefficient and is to be determined from the Fourier analysis of static wind tunnel tests for the particular bluff body shape. Clearly, from Eqs. 3 and 5 the Fourier variable S_1 must be negative and numerically greater than the drag coefficient for a solution to exist.

SQUARE SECTION

The galloping of the square section cylinder has received much attention in the literature. The lift and drag coefficients were measured under the study by Richardson (1965) and repeated here as Fig. 1. The data may be converted to the dimensionless force coefficient. These tests were made at relatively high Reynolds numbers, compared with Mukhopadhyay (1976). While the shape of the lift and drag curves are comparable, the maximum lift coefficients differ by a factor of two. Drag coefficients are comparable. Reynolds numbers differ by an order of magnitude.

To illustrate the use of Eq. 4, four numerical values for peak dynamic angle of attack are assumed, zero, 20, 26, and 30°. The drag is fixed at the average value of $C_D = 1.72$, while the Fourier term S_1 depends on the angle of attack maximum. A sample of the wave form of lift coefficient is shown

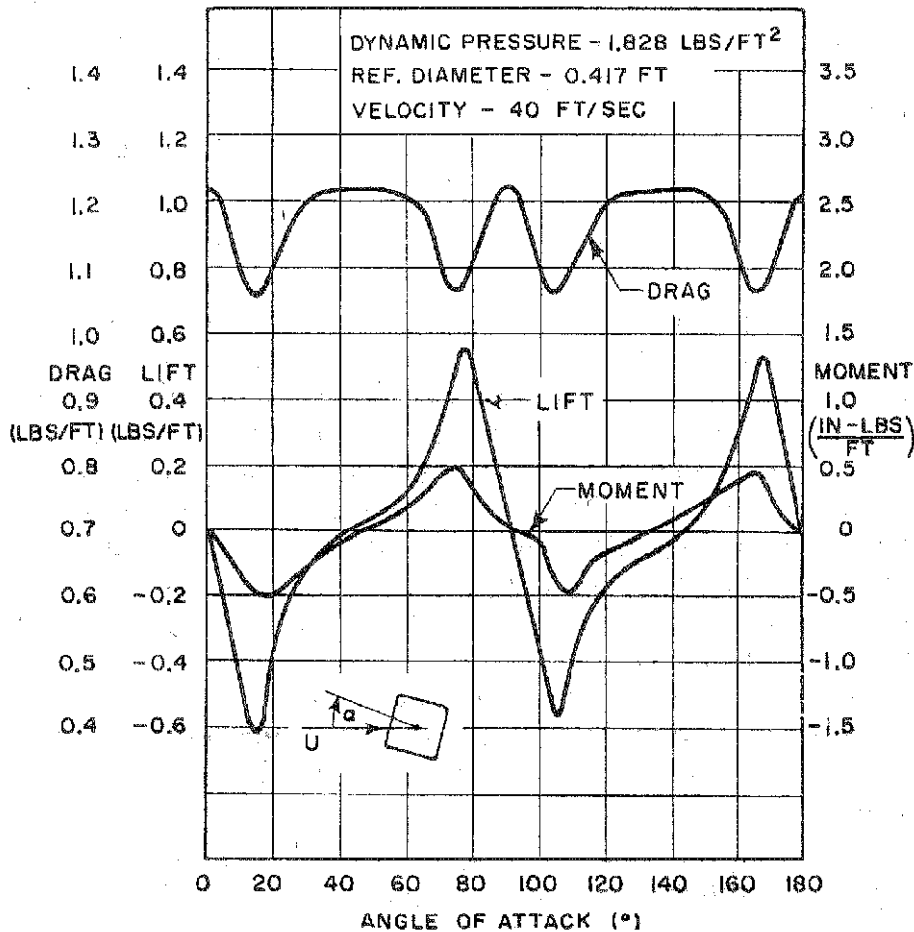


FIG. 1. Square Section Wind Tunnel Data

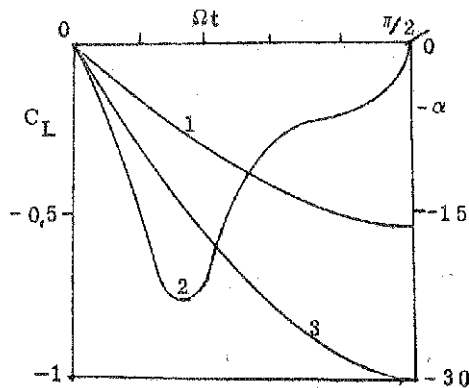


FIG. 2. Dynamic Lift Coefficient C_L ; 1 = First Harmonic Component, $S_1 = 0.55$; 2 = Five-Term Fourier Representation, C_L ; 3 = Negative Angle Of Attack (In Degrees)

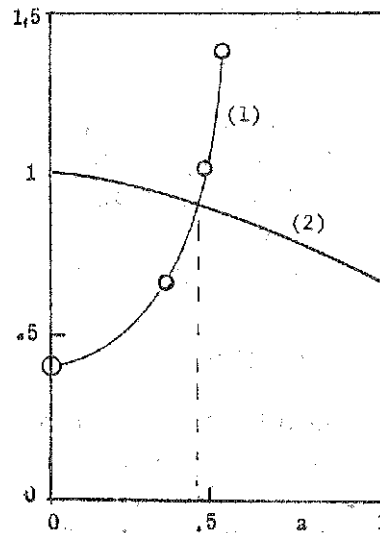


FIG. 3. Solution of Eq. 4 for Square Section; 1 = Left-Hand Side of Eq. 4; 2 = Right-Hand-Side of Eq. 4; Dashed Line Is Solution Point, $a = 0.43$

TABLE 1. Comparison of Galloping Results for Square

Investigator (1)	(a) max (deg) (2)	Reynolds number range (3)
Dugundji et al.	15-22	1,800-3,100
Parkinson et al.	16	5,000-20,000
Ericsson (limit case)	21	Not specified
Richardson et al.	23	100,000

in Fig. 2 for a one-quarter cycle. While five harmonic components are used to reconstruct the wave shape, only the first component (S_1) is of interest here. The reason that such an approximation is permissible is simply because the system may be lightly damped (mechanically) and thus serves as a low-pass filter to higher harmonics of force. The graphical equivalent of Eq. 4 is shown in Fig. 3. The intersection of the two functions defines the stable limit cycle for angle of attack. Once the angle of attack is known, the peak dynamic amplitudes may be calculated from the frequency and wind speed. It is of interest to compare the results of the various investigators (see Table 1).

The prediction technique here illustrated could be used to modify the Fourier component S_1 by reducing the maximum lift coefficient according to the Reynolds number of interest. This would result in a smaller predicted (a)max.

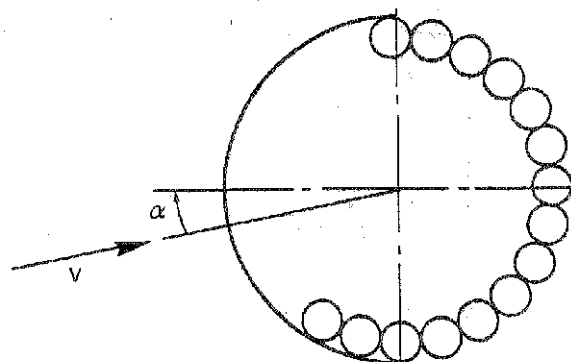
ICED CONDUCTOR SHAPE

While the square has been extensively studied in the literature, an abiding concern exists for the practical consequences of galloping on iced

overhead power line conductors. If aerodynamic data are available for such shapes, the same technique may be applied to estimate maximum dynamic angle of attack.

Fig. 4 is an illustration of recent wind tunnel tests performed in Holland. The simulated ice shape is seen to comprise a zero thickness layer on half of the conductor. There is a strong effect of Reynolds number on the lift coefficient and a lesser effect on the drag coefficient (Hack 1981). Fig. 5 shows other results of a lightly iced conductor (Richardson 1986). The Reynolds number is about 100,000. The thickness of simulated ice is 10% of the conductor diameter. No strands are included, as in Fig. 4.

Both of these aerodynamic shapes may be readily studied by the present



- Δ $V = 4.23\text{m/s}$, $Re = 1.8 \cdot 10^4$
- \circ $V = 8.53\text{m/s}$, $Re = 3.6 \cdot 10^4$
- $+$ $V = 12.87\text{m/s}$, $Re = 5.4 \cdot 10^4$

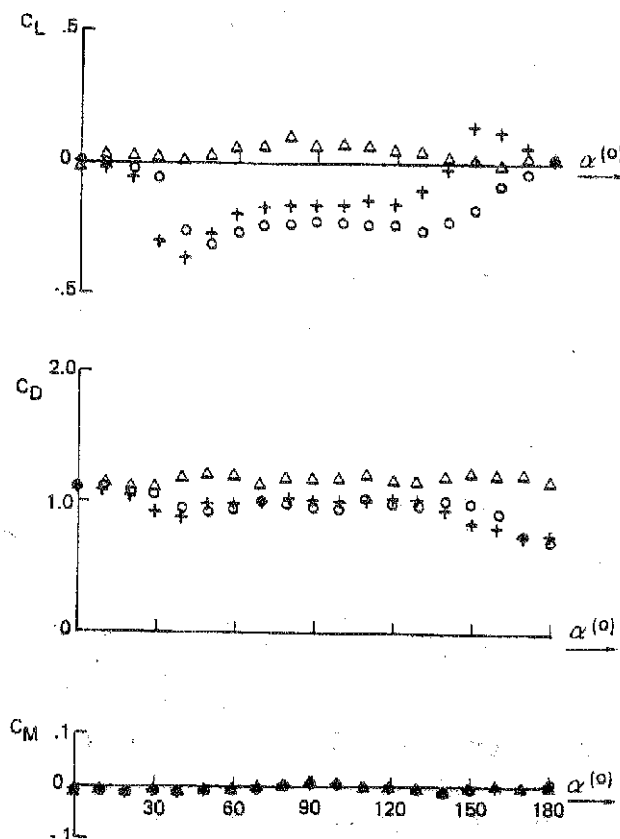


FIG. 4. Measured Aerodynamic Coefficients of Model 3, Half-Smooth Cylinder

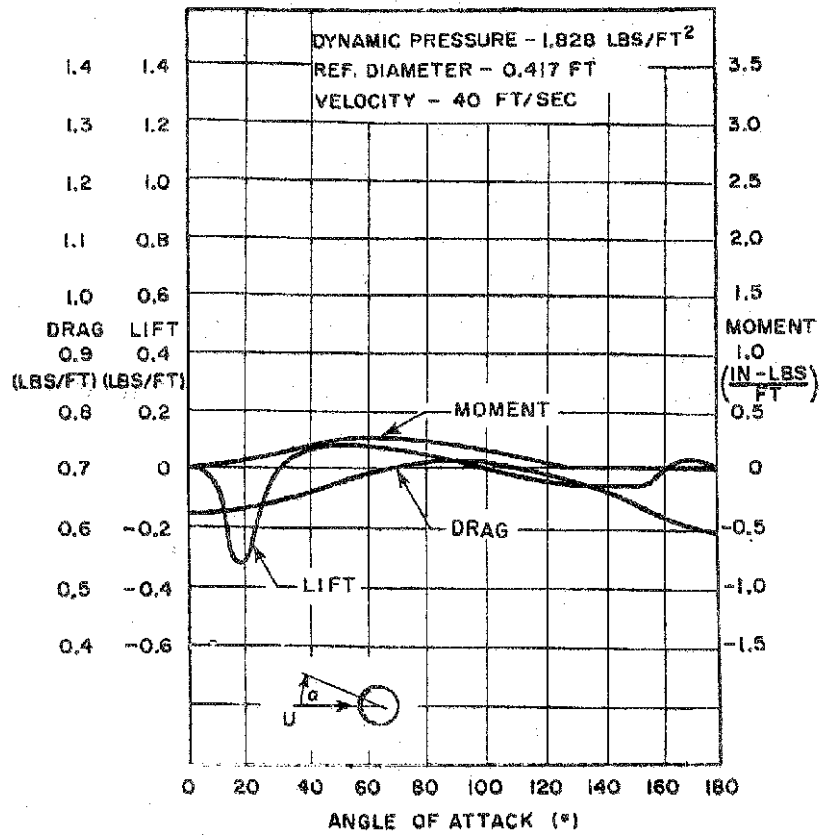


FIG. 5. Aerodynamic Characteristics of Light Ice

method. In the case of the half-smooth conductor, this appears to be a "hard oscillator" such as the D-section shape. Some initial motion is required to get it over the angle of attack threshold. Once that initial motion is supplied, the lift wave form can be approximated by a square

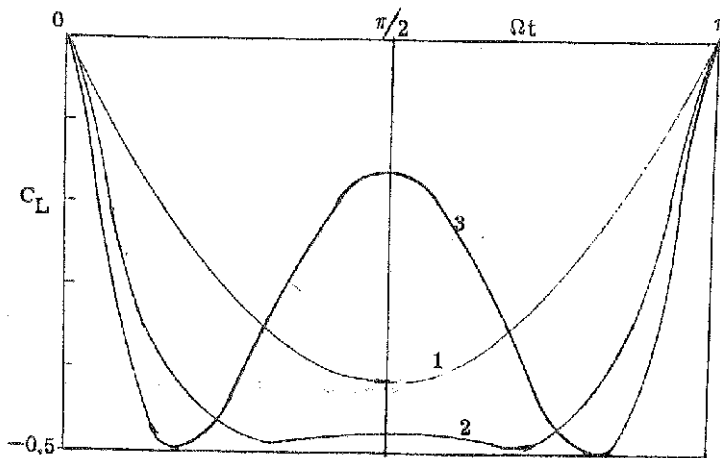


FIG. 6. Dynamic Lift Coefficient for Light Ice; 1 = Maximum Angle of Attack = 11°; 2 = Maximum Angle of Attack = 21°; 3 = Maximum Angle of Attack = 27°

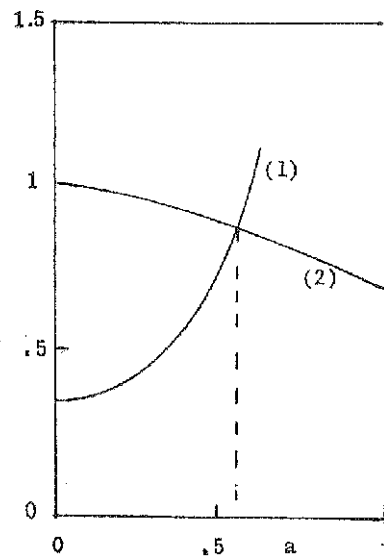


FIG. 7. Solution of Eq. 4 for Light Ice on Conductor; 1 = Left-Hand Side of Eq. 4; 2 = Right-Hand Side of Eq. 4; Dashed Line Is Solution Point $a = 0.52$

wave with dead bands. Such wave form may be readily broken into its Fourier components, and the S_1 term used in the analysis.

Many reports of galloping conductors have stated that very little ice is on the galloping wire, often only a few millimeters in thickness. Yet, as may be seen from the Fig. 5, there is a band of angle of attack over which the lift changes dramatically. This is sufficient to sustain the large amplitudes of gallop that have been observed and reported (EPRI 1980).

The analysis of the Fourier components proceeds from the specification of the wave form, Fig. 6, but only the first harmonic is retained as before. Then a number of different values for the $(a)_{\max}$ are identified and the curves are plotted representing Eq. 4. This procedure leads to Fig. 7. The final value of $(a)_{\max}$ represented by the intersection of curves is $a = 31^\circ$. Ericsson (1983) found a numerical value of $a = 32^\circ$ for the maximum possible gallop.

CONCLUSION

This paper has illustrated a convenient means to estimate gallop amplitude based on known or estimated aerodynamic lift and drag coefficient data. It appears that when the Reynolds number has an effect on such data, the method can easily accommodate such effects without resorting to lengthy and tedious curve-fitting procedures. The effect of mechanical damping will be studied in a future paper.

APPENDIX I. BESSELL FUNCTIONS

TABLE 2. Bessel Functions Used in Analysis

ARG (1)	J_1 (2)	$J_0 - J_2$ (3)	J_0 (4)
0	0	1	1
0.1	0.0499	0.996	0.997
0.2	0.0995	0.986	0.99
0.3	0.1483	0.966	0.977
0.4	0.196	0.941	0.96
0.5	0.2423	0.908	0.938
0.6	0.2867	0.869	0.912
0.7	0.329	0.823	0.881
0.8	0.3688	0.771	0.846
0.9	0.4049	0.712	0.807
1.0	0.4401	0.6502	0.7652
1.1	0.4709	0.583	0.719
1.2	0.4983	0.512	0.671
1.3	0.522	0.437	0.62
1.4	0.5419	0.361	0.568
1.5	0.5579	0.279	0.511
1.6	0.5699	0.199	0.455
1.7	0.5778	0.116	0.397
1.8	0.5815	0.033	0.339
1.9	0.5812	-0.048	0.281

Note: From Jahnke and Emde (1945).

APPENDIX II. REFERENCES

- Egbert, R. I. (1985). "Estimation of maximum amplitudes of conductor galloping by describing function analysis." *IEEE 85 WM 202-7*, IEEE, New York, N.Y.
- Ericsson, L. E. (1983). "Limit amplitude of galloping cables." *AIAA 83-0132*, Amer. Inst. Aeronaut. and Astronautics Meeting, Jan.
- Hack, R. K. (1981). "A wind-tunnel investigation of four conductor models with simulated ice deposits." *NLR TR 81076L*, National Aerospace Laboratory NLR, The Netherlands.
- Jahnke, E. and Emde, F. (1945). *Tables of Functions with formulae and curves*. 4th ed., Dover Publications, New York, N.Y.
- Mukhopadhyay, V. and Dugundji, J. (1976). "Wind-excited vibration of a square section cantilever beam in smooth flow." *J. of Sound and Vibration*, 45(3), 329-339.
- Mukhopadhyay, V. and Dugundji, J. (1978). "Addendum—wind-excited vibration of a square section cantilever beam in smooth flow." *J. of Sound and Vibration*, 56(2), 309-311.
- Parkinson, G. V. (1965). "Aeroelastic galloping in one degree of freedom." *1st Symp. on Wind Effects on Bridges and Structures*, 22, London, England, Jun.
- Richardson, Jr., A. S. (1982). "The time-line method for assessing galloping exposure." *IEEE Paper 82 WM 083-4*, IEEE, New York, N.Y.
- Richardson, Jr., A. S. (1986). "Bluff body aerodynamics." *J. Struct. Engrg.*, ASCE, 112(7), 1723-1726.
- Richardson, Jr., A. S., Martuccelli, J. R., and Price, W. S. (1965). "Research study on galloping of electric power transmission lines." *1st Symp. on Wind Effects on Bridges and Structures*, 7, London, England, Jun.
- Transmission line reference book, wind-induced conductor motion*. (1980). Electric Power Research Institute, RP-792, Palo Alto, Calif.

APPENDIX III. NOTATION

The following symbols are used in this paper:

- A = reference area for aerodynamic coefficients;
 a = peak sinusoidal angle of attack;
 C_D = drag coefficient;
 C_L = lift coefficient;
 C_0 = constant term in Fourier expansion;
 C_1 = C_1 cosine term in Fourier expansion;
 E = energy input per cycle from wind;
 J_0, J_1, J_2 = Bessel functions of first kind;
 q = wind dynamic pressure;
 R = ratio, drag coefficient to Fourier lift coefficient;
 S_1 = first Fourier lift coefficient for dynamic lift;
 t = time;
 Y = maximum vertical dynamic displacement;
 y = vertical dynamic displacement;
 α = instantaneous dynamic angle of attack; and
 Ω = radian frequency of simple harmonic motion.